Title
SPECTROSCOPIC INFORMATION FROM HEAVY-ION REACTIONS

Author
Stephens, F.S.

Publication Date
1969-08-01

Presented at the International Conference on
Properties of Nuclear States, Montreal,
August 25-30, 1969

UCRL-18964
Preprint

cy. 2

SPECTROSCOPIC INFORMATION FROM HEAVY-ION REACTIONS

F. S. Stephens

August 1969

AEC Contract No. W-7405-eng-48

cy. 1

UCRL-18964

DISCLAIMER

SPECTROSCOPIC INFORMATION FROM HEAVY-ION REACTIONS*

F. S. Stephens

Lawrence Radiation Laboratory
University of California
Berkeley, California 94720

August 1969

Abstract

The general subject of spectroscopic studies following heavy-ion reactions is briefly outlined, followed by a more detailed evaluation of the (HI,xn) reactions for such studies. This type of reaction provides a unique opportunity for the systematic study of high angular momentum states. Examples of the types of spectroscopic information obtained using (HI,xn) reactions are presented.

*Work performed under the auspices of the U. S. Atomic Energy Commission.

SPECTROSCOPIC INFORMATION FROM HEAVY-ION REACTIONS*

F. S. Stephens

Lawrence Radiation Laboratory
University of California
Berkeley, California 94720

August 1969

1. Introduction

The general subject of spectroscopic information from heavy-ion reactions is a considerably larger one than can be covered here. Therefore, although the present discussion will be started from a reasonably general point of view, it will rather quickly be confined to a particular type of heavy-ion reaction--the (HI,xn) reaction. Furthermore, no real attempt will be made to cover systematically all the activity going on even in this limited area. The intent is rather to give an overall view first of the (HI,xn) reactions, and then of the types of spectroscopic studies being made using them.

2. Heavy Ion Reactions

The term "heavy ion", will generally be taken to mean projectiles heavier than alpha particles, although in the many instances where alpha particles, or even protons, behave similarly to the heavier projectiles, they are included in the discussion. When a target nucleus is struck by a heavy ion, four types of reaction can occur. Examples of these types for the system $^{40}Ar + ^{124}Sn$ are:

---

*Work performed under the auspices of the U. S. Atomic Energy Commission.

1) $^{40}Ar + {}^{124}Sn \longrightarrow {}^{40}Ar' + {}^{124*}Sn$

2) $^{40}Ar + {}^{124}Sn \longrightarrow {}^{39*}Cl + {}^{125*}Sb$

3) $^{40}Ar + {}^{124}Sn \longrightarrow {}^{164*}Er$

4) $^{40}Ar + {}^{124}Sn \longrightarrow$ fragmentation .

These reactions are listed generally in order of increasing bombarding energy. The first includes both Coulomb excitation and nuclear inelastic scattering and results in excitation of the target (and/or projectile) nucleus. The second involves the transfer of one or several nucleons between target and projectile and generally results in excitation of both product nuclei. The third involves compound nucleus formation, and typically leaves the compound nucleus in a very highly excited state. The many more-complex possibilities occurring at higher bombarding energy are lumped together in the fourth category. For the present purposes these are simply characterized by the break-up of the system into several product fragments.

There are fairly obviously two types of spectroscopy that can be applied to these heavy-ion reactions. The first is charged-particle spectroscopy which involves analysis of the energy of the outgoing (usually light) particle(s). The power of this method lies in the fact that the discrete lines in the energy spectrum give directly information on particular energy levels in (generally) the target nucleus. This method is applicable to reaction types 1) and 2) above, where a single light charged particle emerges, but is obviously not applicable to types 3) and 4). Enormous quantities of information have been obtained with light projectiles (protons to alpha particles) using this method. However, for heavy ions, this form of spectroscopy becomes much more difficult. Although charged-particle spectroscopy with heavy ions seems likely to become increasingly important, it will not be discussed here.

The second type of spectroscopy is concerned with the gamma rays and conversion electrons emitted in the deexcitation process following reactions induced by heavy ions. In order that the spectra obtained in this case be reasonably simple to interpret, they must result from conditions where there is a single dominant reaction product. There are two ways to achieve this. The first is to combine the two types of spectroscopy by looking at the gamma rays or conversion electrons in coincidence with emitted charged-particle groups, and the second is to choose bombarding conditions where the cross section leading to a particular product nucleus is a large fraction of the total cross section. The coincidence technique is powerful because one can observe separately the radiations coming from each level of a given product nucleus; however, little work of this type has been done so far with heavy ions. On the other hand many electron and gamma-ray spectroscopic studies have been made under bombarding conditions where a single product dominates. The two such conditions heavily exploited are Coulomb excitation, which is the only reaction occurring below the Coulomb barrier, and the compound nucleus reactions, which dominate the total reaction cross section at energies moderately above the Coulomb barrier. The rest of the present discussion will be concerned primarily with the compound nucleus reactions.

In fig. 1 a schematic view of a ^{124}Sn nucleus is shown as seen by an incoming 160 MeV ^{40}Ar projectile. The figure illustrates the prominent reactions that can occur together with their relative cross sections and (idealized) impact parameters. Only Coulomb excitation can occur if the target and projectile do not come into contact with each other; surface reactions, consisting largely of nuclear inelastic scattering and transfer reactions, happen at

grazing distances; and compound nucleus formation dominates within a certain impact distance. Furthermore, the compound nucleus decays in several ways depending on the impact parameter, or angular momentum of the system. For large angular momenta ($\gtrsim 50\ \hbar$ in this case) alpha particles are emitted together with neutrons, as the heavier alphas are better able to carry off angular momentum. Below $\sim 50\ \hbar$ mainly neutrons are emitted, the number of which again depends on angular momentum, as will be discussed later. These are called the (HI,xn) reactions. As shown in fig. 1 (and experimentally measured[1]) for this particular case) about one third of the total reaction cross section is going into the (^{40}Ar,4n) reaction, which is sufficient to make gamma-ray and electron spectroscopic studies possible. If a lighter projectile such as ^{4}He is used, then the angular momentum effects are much smaller and essentially the entire compound nucleus cross section can go into a particular reaction--e.g., the (^{4}He,2n) reaction on heavy target nuclei at 25 MeV--producing cleaner spectra.

Two additional points should be emphasized about fig. 1. The first is that increasing the bombarding energy causes more neutrons (or charged particles) to be emitted and also decreases the specificity of the reaction. Thus the (HI,xn) reactions are rarely useful for this type of spectroscopic study at energies where more than ~ 6 neutrons are emitted. The picture (fig. 1) also changes as the neutron number of the target changes, due to differences in the neutron and alpha-particle (or proton) binding energies. As the target gets more neutron deficient the neutron binding energy goes up whereas the alpha-particle (and proton) binding energies go down, resulting in more charged-particle emission. Eventually a point comes where the xn reactions no longer dominate, and the gamma-ray and electron spectra are no longer simple to interpret.

This raises the question of what regions of the periodic table are subject to such spectroscopic studies following (HI,xn) reactions. This is shown in fig. 2, which is a chart of the stable nuclides (squares), with the magic numbers shown as light solid lines, and the neutron and proton drip lines shown as heavy solid lines. The dashed line encloses the region where one would expect these spectroscopic studies following (HI,xn) reactions to be relatively easy. It is bounded at the low mass number end by the development of a sufficiently large Coulomb barrier to prevent charged particle emission and at the high mass number end by fission competition. The neutron rich side is determined by available target nuclei--using (α,2n) reactions; whereas, the neutron deficient side is limited by the onset of charged-particle emission as discussed above. Approximately 1000 nuclei lie in this region, of which perhaps 200 have currently had some study using this method. Also indicated on fig. 2 are the regions of nuclei that can be made by (^{4}He,2n) reactions (orange) and by (^{40}Ar,4n) reactions (green). It is apparent that almost the entire (HI,xn) region can be covered using projectiles up to ^{40}Ar. Thus the availability of projectiles heavier than ^{40}Ar will not greatly increase the number of nuclei subject to (HI,xn) spectroscopic studies of this type, although it will aid these studies enormously in other ways. It should be emphasized, however, that the region between the dashed line and the proton drip line is potentially available to spectroscopic studies if a particular product can be singled out. Spectra taken in coincidence with the emitted alpha particles and protons might yield enough additional information to make somewhat more of this region usable.

The next few paragraphs will examine the kinds of gamma ray cascades that follow (HI,xn) reactions. The ideas presented are extensions[2]) of a model discussed recently by Grover et al.,[3]) and in some places are not completely established, though they are consistent with a large body of data. Figure 3 is a plot of excitation energy in an even-even nucleus with mass number around 160 versus angular momentum. The light line traces out the quasi-particle levels of lowest energy with a given angular momentum. Such levels are called by Grover the yrast levels. At the lowest angular momenta, the levels of the ground-state collective band are the yrast levels, and the dots and dashes indicate such levels for a vibrational and rotational nucleus, respectively. The two heavy lines indicate the average excitation energies and angular momentum ranges populated in this nucleus following neutron evaporation from (^{4}He,4n) and (^{40}Ar,4n) reactions. For the (^{4}He,4n) reaction, essentially the entire angular momentum range possible in compound nucleus formation is represented. The (^{40}Ar,4n) range, however, is limited on the high angular momentum side by failure to emit the fourth neutron (due to lack of enough final states with sufficient angular momentum), and on the low side by the emission of a fifth neutron. The gamma-ray deexcitation following both types of reaction probably begins with the emission of a few high energy transitions down to the vicinity of the yrast levels, but then the two types of reaction differ. For the (^{4}He,4n) reaction a typical pathway according to Halpern and co-workers[4]) might then involve several transitions in a collective band based on some quasi-particle or vibrational state before population of the ground-state collective band occurs. Thereafter deexcitation to the ground state is via the ground-state band; and, since this portion of the deexcitation is common to all pathways,

the transitions in the ground-state band stand out as (often the only) strong discrete lines in the spectra. For the (^{40}Ar,4n) reaction the subsequent deexcitation differs in that some 20 $\hbar$ of angular momentum must be lost before the ground band can be populated. The evidence suggests that the population cascades down reasonably close to the yrast line, and then feeds rather sharply into the ground band at the point where it becomes lowest in energy.

The important feature of the deexcitation process outlined for the heavy projectiles, is that the lowest-lying high-angular-momentum states are systematically populated. For spectroscopic studies this means two general things. First, for $I \lesssim 12$ discrete high-spin states in the ground band (or other low-lying bands in odd-mass and odd-odd nuclei) will be systematically heavily populated. These levels are then available for a variety of spectroscopic measurements, and most of the work in (HI,xn) reactions to date has involved study of them. However, a second possibility is to study the deexcitation to learn about the regions of higher angular momentum. For example, in even-even nuclei the point where the population converges from many bands into the ground band, is likely to be where the ground band becomes energetically favored over the other bands. Thus it may be indicating the point where the energy gap develops, and this can perhaps give some information on the behavior of the pairing correlations as a function of angular momentum. Also, recent measurements[5]) have shown that the mean time elapsed between the reaction and population of the ground band in three (^{40}Ar,4n) reactions is only $\sim$10 psec. This rapid deexcitation probably indicates the presence of collective bands in the yrast region. Thus it seems that these (HI,xn) reactions may serve as a unique means to study states of very high angular momentum.

3. Spectroscopic Information from (HI,xn) Reactions

There are three properties of (HI,xn) reaction products that make them extremely useful for spectroscopic studies. These are:

1) high angular momentum

2) large, uniform recoil velocity

3) alignment of angular momentum .

The previous discussion has shown why the (HI,xn) reactions systematically populate states of high angular momentum. For the spectroscopist this first property has thus far meant that he has a method for producing systematically high-spin rotational or vibrational states for study. The fact that no high-energy heavy particles are emitted from the compound nucleus means that it has essentially the full momentum of the incoming projectile. The products thus recoil at high velocity along the beam direction--property 2) above. This has been used in a variety of ways, three of which are: 1) as a clock, by converting the measurement of distance into time; 2) as a means for getting the product nucleus rapidly into a desired environment--implantation; and 3) as a means to produce very large magnetic fields. Finally, it is well known that the orbital angular momentum brought into the nucleus is aligned in the plane perpendicular to the beam direction, giving rise to property 3). This means that the emitted radiations are anisotropic and their angular distributions, relative to the beam direction, contain information about the multipolarities of the transitions and the spins of the levels involved. The alignment can also serve as a tag to measure the effect of a perturbing magnetic or electric field. These three properties make the (HI,xn) reactions a very useful spectroscopic tool, as the following examples are intended to illustrate.

3.1. Levels in Even-Even Nuclei

The first experimental studies of discrete gamma rays following (HI,xn) were made in 1963 by Morinaga and Gugelot[6]) on the collective (rotational or vibrational) levels of the ground-state bands in even-even nuclei. Most of the work since then has centered on levels of this type. Figure 4 shows a rather typical Ge(Li) spectrum[7]) following a (^{11}B,4n) reaction on ^{165}Ho. The dominant lines are the rotational transitions in the ground band of ^{172}Hf. The angular distributions of these lines relative to the beam direction are shown in fig. 5, and are all about 50% larger at 0° than at 90°. This is consistent with their assignment as "stretched" (I → I-2) E2 transitions. A recent study of this type submitted to this conference (Contribution 3.4 by A. Hashizume et al.) is shown in fig. 6. Here the even-even Cd nuclei have systematically been made by (^{4}He,xn) and (^{3}He,xn) reactions on the Pd isotopes. This work shows that the method can be applied systematically to many isotopes of a given element, (six in this case without using much variety in projectiles). However, assignments such as these need to be supported by angular distribution and/or coincidence measurements, especially in vibrational nuclei. Rather than surveying the large quantities of recent data of this type, I have chosen to give examples of other types of information coming from (HI,xn) reactions.

3.2. Lifetime Measurements

In fig. 7 is shown a method we have used at Berkeley[5]) to measure lifetimes of levels following (HI,xn) reactions. The method is called the recoil-distance Doppler-shift method, and has been used previously in measurements on very light nuclei. Following the ^{124}Sn(^{40}Ar,4n)^{160*}Er reaction, the ^{160*}Er

nuclei are moving along the beam direction with $v/c \approx 2\%$. A lead plunger stops them a given distance away from the target. If an ^{160*}Er nucleus emits a gamma ray while it is moving, it gives a Doppler shifted line in a Ge(Li) detector placed at 0° relative to the beam direction. If it is stopped in the lead plunger, it gives an unshifted line. The lead plunger is attached to a micrometer and spectra taken at a number of distances are shown in fig. 8. At the top of fig. 8 the distance between target and plunger is small, and the lines (corresponding to rotational transitions in ^{160}Er) are mostly unshifted; whereas at the bottom the distance is larger and the lines are all completely shifted. A nice feature of this method is that the separation between the shifted and unshifted lines immediately gives the velocity of the recoiling Er nuclei. At each distance the fraction of each line that is unshifted is calculated and this quantity is plotted against plunger distance in fig. 9. Here the points for each transition are fitted to equations that take account of the sequential nature of the cascade. The lifetime for a given level must simultaneously fit both the change in slope and the displacement in distance from the previous transition. Two kinds of information come from these measurements. The first is half-life information for the various rotational levels. The longest transition shown here ($4 \rightarrow 2$) has a half-life of $\sim$35 psec and could be measured to an accuracy of $\sim$5%. This varied down to the shortest transition ($10 \rightarrow 8$) whose half-life of $\sim$1 psec was measured to within $\sim$40%. Such data are relevant to considerations of centrifugal stretching or Coriolis anti-pairing that may be occurring in these bands, but will not be discussed further here. The other kind of information is the mean elapsed time between the reaction (zero distance) and the top of the ground state band ($\sim$10 - 8 transition here).

As previously indicated, this gives information about the very high angular momentum states in these nuclei.

3.3. Perturbed Angular Distributions

The subject of perturbed angular distributions is a very large one, and I have neither the space nor background to give a review of it. However, the (HI,xn) reactions are so admirably suited to these studies that some description of the subject seems essential. Figure 10 gives an introduction to the magnetically perturbed angular distributions. The first two vertical lines indicate the magnetic fields necessary to cause an easily observable perturbation ($\omega\tau \times 0.1$) in states having a g factor of 0.3 and various mean lifetimes. It is seen that for mean lifetimes longer than 10 nsec, the required fields are less than 10 kG, which are easy to produce. In fact for such cases the problem is rather to prevent some extraneous field from causing unwanted perturbations. For short lifetimes, however, large fields are required (and if a g factor is to be measured, such fields must be produced)--e.g., around 100 MG for a 1 psec state. The third group of four vertical lines in fig. 10 indicates methods to produce magnetic fields for these studies. The rf fields, which make possible very precise NMR measurements[8]), can be produced up to 10 G or so ($\tau \sim 10^{-5}$ sec) with a possible extension of about a factor of 1000 due to the hyperfine enhancement obtained in ferromagnetic materials. Conventional magnets (second line) can be used to perturb states down to $\tau \sim 10^{-9}$ sec. For still higher fields two other techniques are known, both of which make use of the recoil velocity of the (HI,xn) reaction products. The first of these is implantation in a magnetized ferromagnetic material[9]), where in some cases,

fields of several MG can be obtained, and the second is the hyperfine field present in a highly-excited recoiling free ion, which can be 50 MG or larger. The fourth group of lines in fig. 10 show something about producing the oriented nuclei essential to such an experiment. This orientation generally must be preserved for times comparable to the lifetime of the level under study if an appreciable perturbation in the angular distribution is to be observed. For lifetimes in the minute range or longer, one can use low temperature techniques (or others) to produce and maintain the orientation. For the reactions the nuclei are initially oriented, and the problem is simply to preserve this orientation for a time comparable with the lifetime of the state under study. This is relatively easy to do for times shorter than $\sim$1 nsec, moderately difficult for times up to $\sim$1 μsec, and generally quite difficult for longer times. Angular correlations with radioactive sources and Coulomb excitation are methods in principle very similar to the reactions for orienting nuclei; however, random coincidences and vanishing probabilities for excitation limit these methods, in practice, to times shorter than about 1 μsec and 10 nsec, respectively.

The attractive region for perturbed angular distribution or correlation measurements is from about 10 psec to 1 μsec, where preservation of the alignment is not too difficult, and magnetic fields are available either from conventional magnets or by implantation. Many states have been measured in this time range mostly using the angular correlation or Coulomb excitation techniques. In Contribution 4.9 to this conference Yamazaki *et al.* have measured the g factor of a 110 nsec state in ^{210}Po following a (^{4}He,2n) reaction on ^{208}Pb. One can see from fig. 10 that the reactions alone offer general access to the region

from ∿1 μsec to several seconds for perturbed angular distribution studies. Preserving the orientation in this time range is difficult, but NMR studies have been made in both the minute and the msec regions by Sugimoto et al.[10]) and very recently in the 10 μsec region by Quitmann et al.[11]). Another recent measurement in the 10 μsec region by Christiansen et al.[12]) used a magnet to produce the perturbing field and a clever detection technique called "the stroboscopic method". At the opposite end of the time range are the experiments of Ben Zvi et al.[13]), who recoiled Coulomb excited nuclei into vacuum (and gas) and observed hyperfine fields of around 25 MG. They measured perturbations in states with lifetimes down to 2 psec. At Berkeley (Contribution 4.10, R. Nordhagen et al.) we have applied this technique to (^{40}Ar,4n) products where the higher recoil velocity gives larger fields--up to about 50 MG. It is amusing to note that in these cases the reaction essentially produces the states for study, aligns them, puts them into a suitable environment (vacuum), and produces the magnetic field to perturb them. (Unfortunately it does not write the paper, however.) This seems like a widely applicable technique, though it is far from completely understood at present.

These perturbed angular distribution techniques seem very powerful both for measuring nuclear g factors and for studying the properties of hyperfine fields. Probably application can also be made to nuclear electric quadrupole moments and electric field gradients.

3.4. Odd-Mass Nuclei

Although most (HI,xn) work to date has centered on even-even nuclei, there is now a rapidly increasing amount of data on odd-mass nuclei. Information

on some odd-mass Er isotopes, somewhat arbitrarily chosen to illustrate this work, is shown in fig. 11. On the left is the level scheme of ^{161}Er as given by Hagemann, et al.[14]) (with some of the rotational transitions omitted). This case was chosen because it has two especially interesting features. The first is the 8 μsec, 11/2 - [505] state which comes up into this region from the 50-82 neutron shell. These levels are useful in relating the two major shells energetically, and using the presently-described techniques, Borggreen and Sletten[15]) have observed this level in 6 or 8 nuclei in this region. The second interesting feature is the strong cascade of transitions shown on the extreme left. This sequence of transitions resembles an even-even cascade, both in energy and in that they are the strongest lines in the spectrum and have angular distributions indicating a "stretched" E2 character. The interpretation given by the Swedish group is that these are members of the 1/2 + [660] band, which has a decoupling parameter around 9. At Berkeley[16]) we have seen similar sequences of transitions in ^{159}Er and ^{157}Er in conjunction with our studies of even-even Er nuclei in this region. These levels are shown on the right of fig. 11, arbitrarily placed in energy since we have not untangled the bottom of the scheme. The reason for including these cases is that, due to the heavy projectile, we have been able to measure the lifetime of the (presumed) $17/2^+$ level in ^{157}Er by the recoil-distance method, and find that it corresponds to an enhancement of about 40 for an E2 transition, in agreement with the expected collective character. By recoiling ^{157}Er into vacuum the g factor was also found to be very small (±0.05±0.05), consistent with the expectations for the 1/2 + [660] state. I believe the Swedish group also has information on ^{163}Er and ^{165}Er, making a total of at least five Er nuclei in

which this band can be studied. It is expected to be strongly Coriolis coupled to other levels from the $i_{13/2}$ orbital, and should provide an excellent opportunity to study such couplings.

The odd-odd nuclei are also subject to studies of this type, and although their added complexity has made them initially less attractive to study than the even-even or odd-mass types, this situation will surely not persist.

3.5. Out-of-Beam Studies

There are really three time intervals to consider in spectroscopic studies following (HI,xn) reactions. Figure 12 illustrates this point. Many accelerators are pulsed, and the beam occurs in bursts whose length, in most cases, ranges from ∿1 nsec to ∿5 msec. Radiations occurring in this period are considered "prompt", and most of the work discussed thus far has been on radiations of this type. However, there are also intervals between the beam bursts (in most cases ∿10 nsec - ∿100 msec) where radiations with long enough half-lives can be studied with much less background radiation than during the beam burst. Many isomeric states with half-lives longer than a few nsec have been studied in this time region. Thirdly, lifetimes longer than a few seconds can be studied with the accelerator turned off. As a short example, we[17]) were interested in the so-called β-bands in even-even nuclei with neutron number around 90. Systematic comparison of electron and gamma-ray spectra from very short-lived odd-odd nuclei ($t_{1/2}$ = 1-10 min) showed half a dozen cases of monopole transitions around 1 MeV in Dy, Er, and Yb nuclei in this region. Further gamma-ray studies support these β-band assignments. Both the intervals between beam bursts and short beam-off periods were used in these explorations. There is an enormous amount of work of this type that can be done.

4. Conclusion

In summary, an attempt has been made to demonstrate that the (HI,xn) reactions provide a unique opportunity for the systematic study of high angular momentum states, and in addition have other characteristics which greatly aid such studies.

Acknowledgments

I am indebted to Dr. R. M. Diamond for continuing discussions covering all topics mentioned. I should also like to thank him, together with Drs. J. O. Newton, S. Cirilov, and K. Nakai, for their critical reading of this manuscript.

References

1. D. Ward, F. S. Stephens, and J. O. Newton, Phys. Rev. Letters 19 (1967) 1247.
2. F. S. Stephens, R. M. Diamond, W. H. Kelly, J. O. Newton, and D. Ward, to be published.
3. J. R. Grover and J. Gilat, Phys. Rev. 157 (1967) 802; ibid. 814; ibid. 823; J. R. Grover, Phys. Rev. 157 (1967) 832.
4. C. F. Williamson, S. M. Fergusen, B. I. Shepherd, and I. Halpern, Phys. Rev. 174 (1968) 1544.
5. R. M. Diamond, F. S. Stephens, W. H. Kelly, and D. Ward, Phys. Rev. Letters 22 (1969) 546.
6. H. Morinaga and P. C. Gugelot, Nucl. Phys. 46 (1963) 210.
7. J. O. Newton, F. S. Stephens, R. M. Diamond, K. Kotajima, and E. Matthias, Nucl. Phys. A95 (1967) 357.
8. See the review by D. A. Shirley in Magnetic Resonance and Radiofrequency Spectroscopy, ed. by P. Averbuch, Proceedings of the XV^{e} Colloque A.M.P.E.R.E., Grenoble, France, 16-21 September 1968, (North-Holland, Amsterdam, 1969).
9. See the review by L. Grodzins, Ann. Rev. Nucl. Sci. 18 (1968) 291.
10. K. Sugimoto, A. Mizobuchi, K. Nakai, and K. Matuda, Phys. Letters 18 (1965) 38; K. Sugimoto, K. Nakai, K. Matuda, and T. Minamisono, Phys. Letters 25B, (1967) 130.
11. D. Quitmann, J. M. Jaklevic, and D. A. Shirley, Lawrence Radiation Laboratory Report UCRL-18871 (April 1969).
12. J. Christiansen, H.-E. Mahnke, E. Recknagel, D. Riegel, G. Weyer, and W. Witthuhn, Phys. Rev. Letters 21 (1968) 554.
13. I. Ben Zvi, P. Gilad, M. Goldberg, G. Goldring, A. Swarzschild, A. Sprinzak, and Z. Vager, Nucl. Phys. A121 (1968) 592.

14. K. A. Hagemann, S. A. Hjorth, H. Ryde, and H. Ohlsson, Phys. Letters 28B (1969) 661.

15. J. Borggreen and G. Sletten, to be published in Nucl. Phys.

16. R. Nordhagen, R. M. Diamond, G. Goldring, and F. S. Stephens, unpublished data (1969).

17. D. Ward, R. M. Diamond, M. Neiman, and F. S. Stephens, unpublished data (1968).

Figure Captions

Fig. 1. Schematic view of a ^{124}Sn target nucleus as seen by an incoming 160 MeV ^{40}Ar projectile.

Fig. 2. Chart of the nuclides showing the region (enclosed by the dashed line) where spectroscopic studies following (HI,xn) reactions should be relatively easy. Also shown are the regions of product nuclei that can be made by (α,2n) reactions (orange) and (^{40}Ar,4n) reactions (green).

Fig. 3. Schematic figure showing the energy levels in a nucleus of mass $\sim$160 versus angular momentum. Indicated on the figure are 1) the lowest quasi-particle energy levels of a given spin (yrast levels), 2) the region of populated states following (He,4n) and (Ar,4n) reactions, and 3) the ground-band levels of a typical vibrator (dots) and rotor (dashes).

Fig. 4. Typical Ge(Li) spectra obtained at two angles following a (HI,xn) reaction. The dominant lines at both angles are the rotational transitions of ^{172}Hf.

Fig. 5. Angular distributions of the rotational lines observed in Fig. 4. All these distributions show the typical "stretched" (I $\rightarrow$ I-2) E2 pattern.

Fig. 6. Level schemes of the even-even Cd isotopes proposed by Hashizume et al., Contribution 3.4 to this conference.

Fig. 7. Schematic view of the recoil-distance Doppler-shift method for measuring the lifetimes of states in ^{160}Er following (^{40}Ar,4n) reactions on ^{124}Sn.

Fig. 8. Spectra from the ^{124}Sn(^{40}Ar,4n)^{160}Er reaction taken with the plunger set at the indicated distances from the target. The positions of the unshifted (shifted) lines are given at the top (bottom) of the figure.

Fig. 9. The fraction of each transition which is unshifted in energy vs. the separation distance of the target and plunger. The symbols represent experimental points for the ground-band transitions in ^{160}Er. The solid lines are the calculated curves, and the dashed line for the $8 \rightarrow 6$ transition shows the effect of allowing two components to feed the ground-state band.

Fig. 10. The two vertical lines at the left indicate the magnetic field, H, necessary to cause a given perturbation ($\omega\tau = 0.1$) in a state with a g factor of 0.3 and various mean lifetimes (τ). The two groups of lines at the right show methods to produce magnetic fields and oriented nuclei appropriate to states of various τ.

Fig. 11. Level scheme of ^{161}Er (left) showing the 8 μsec 11/2 - [505] state and the extremely anomalous 1/2 + [660] band. At right are the partial schemes of ^{159}Er and ^{157}Er (whose spins are assigned by analogy with ^{161}Er), showing the measured half-life and g factor of one of the levels.

Fig. 12. Schematic illustration of the three time intervals available for spectroscopic studies at a pulsed accelerator.

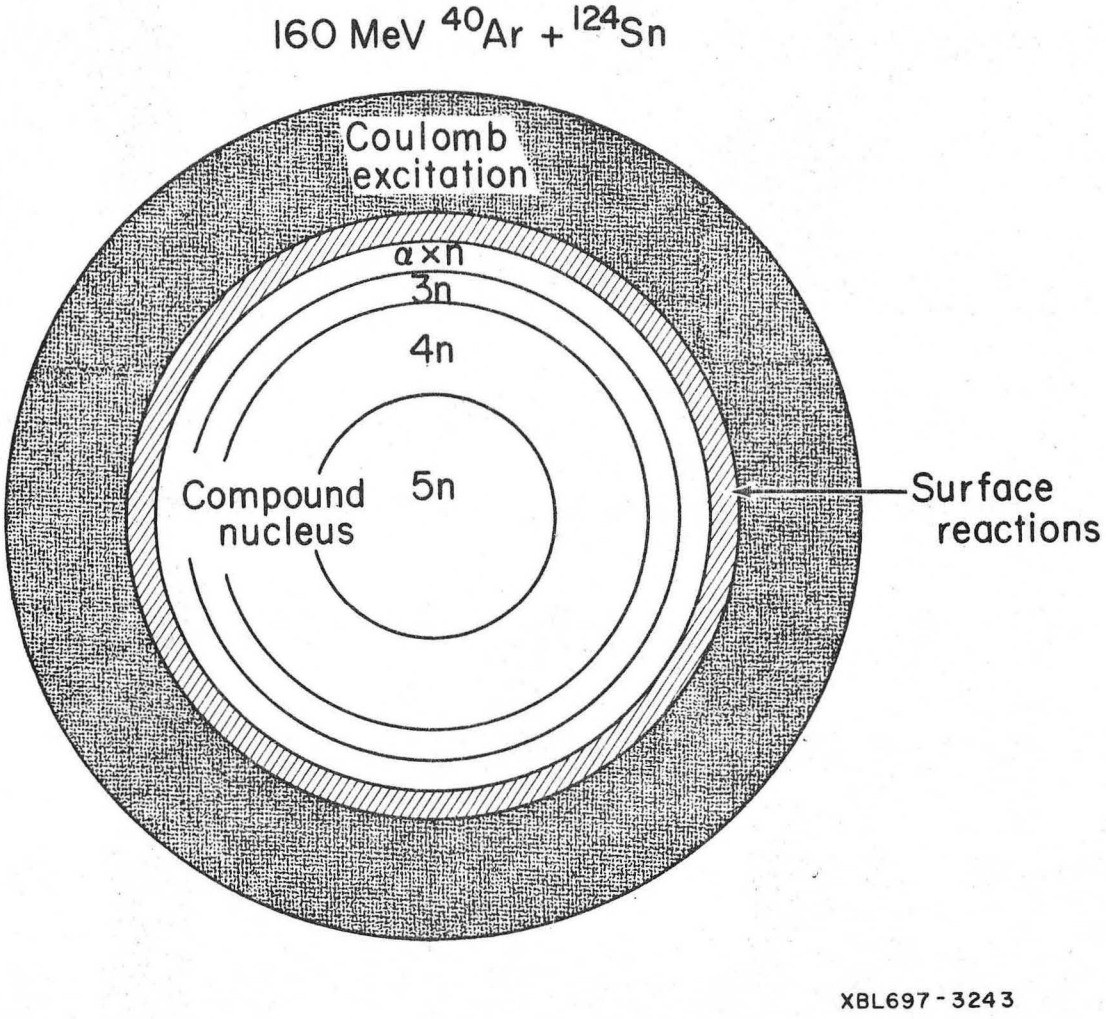
160 MeV ^{40}Ar + ^{124}Sn
Coulomb excitation
α×n
3n
4n
5n
Compound nucleus
Surface reactions
XBL697-3243

Fig. 1

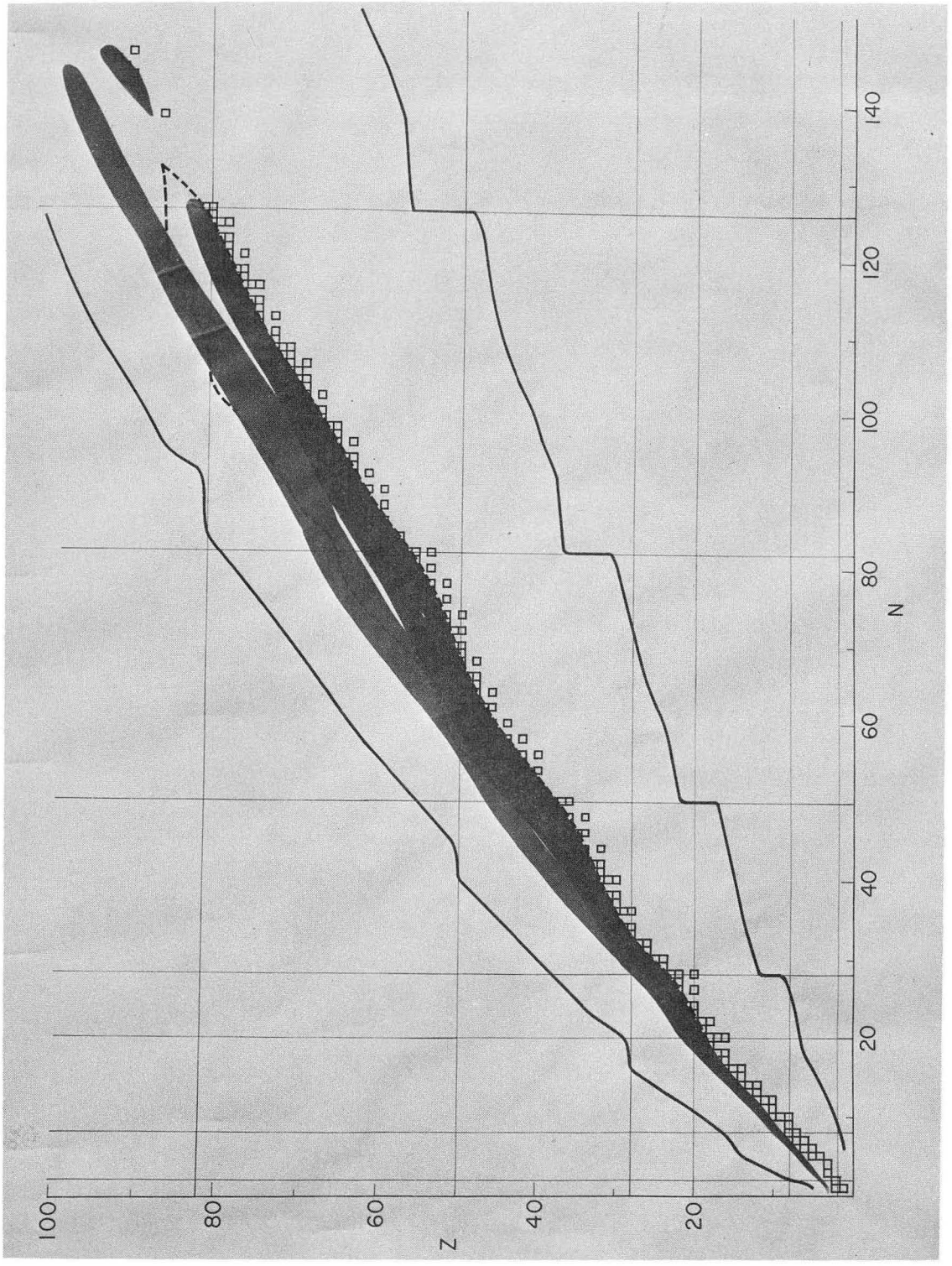

XBC 697-4897

Fig. 2

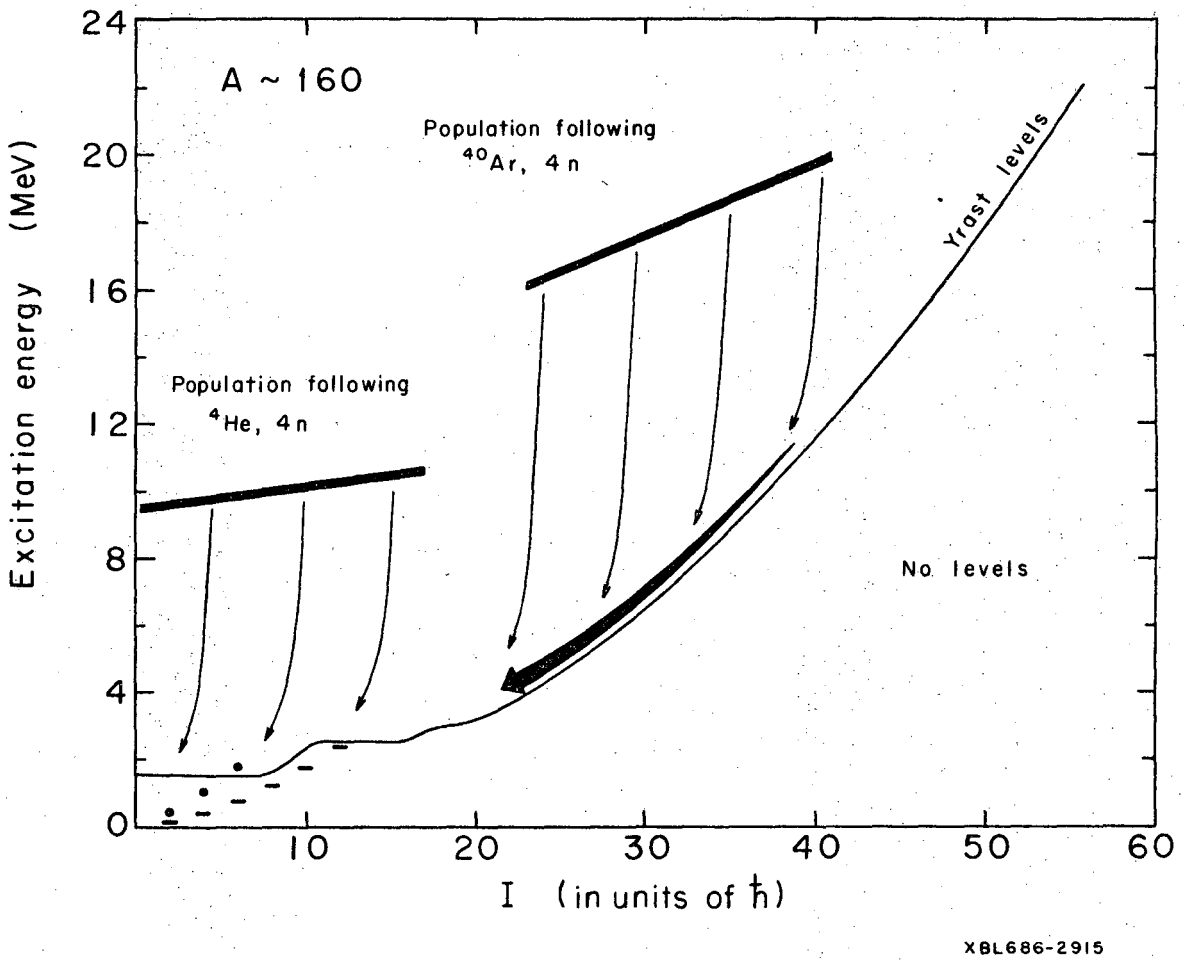
A ~ 160
Population following
^{40}Ar, 4 n
Population following
^{4}He, 4 n
Yrast levels
No levels
Excitation energy (MeV)
I (in units of ħ)
0
4
8
12
16
20
24
10
20
30
40
50
60
XBL686-2915

Fig. 3

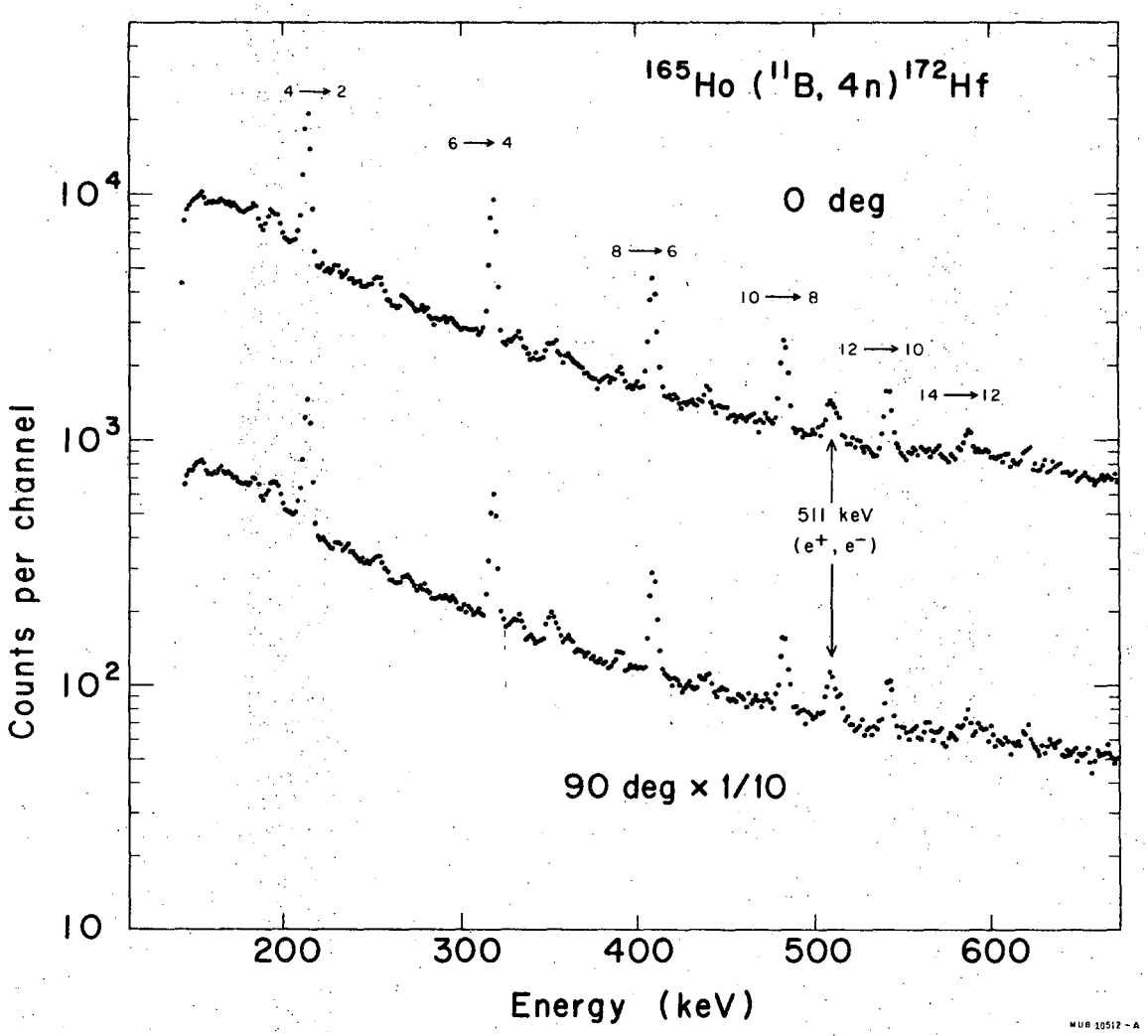
^{165}Ho (^{11}B, 4n)^{172}Hf
4 → 2
6 → 4
8 → 6
10 → 8
12 → 10
14 → 12
0 deg
511 keV
(e$^+$, e$^-$)
90 deg × 1/10
Counts per channel
Energy (keV)
10^4
10^3
10^2
10
200
300
400
500
600
MUB 10512 - A

Fig. 4

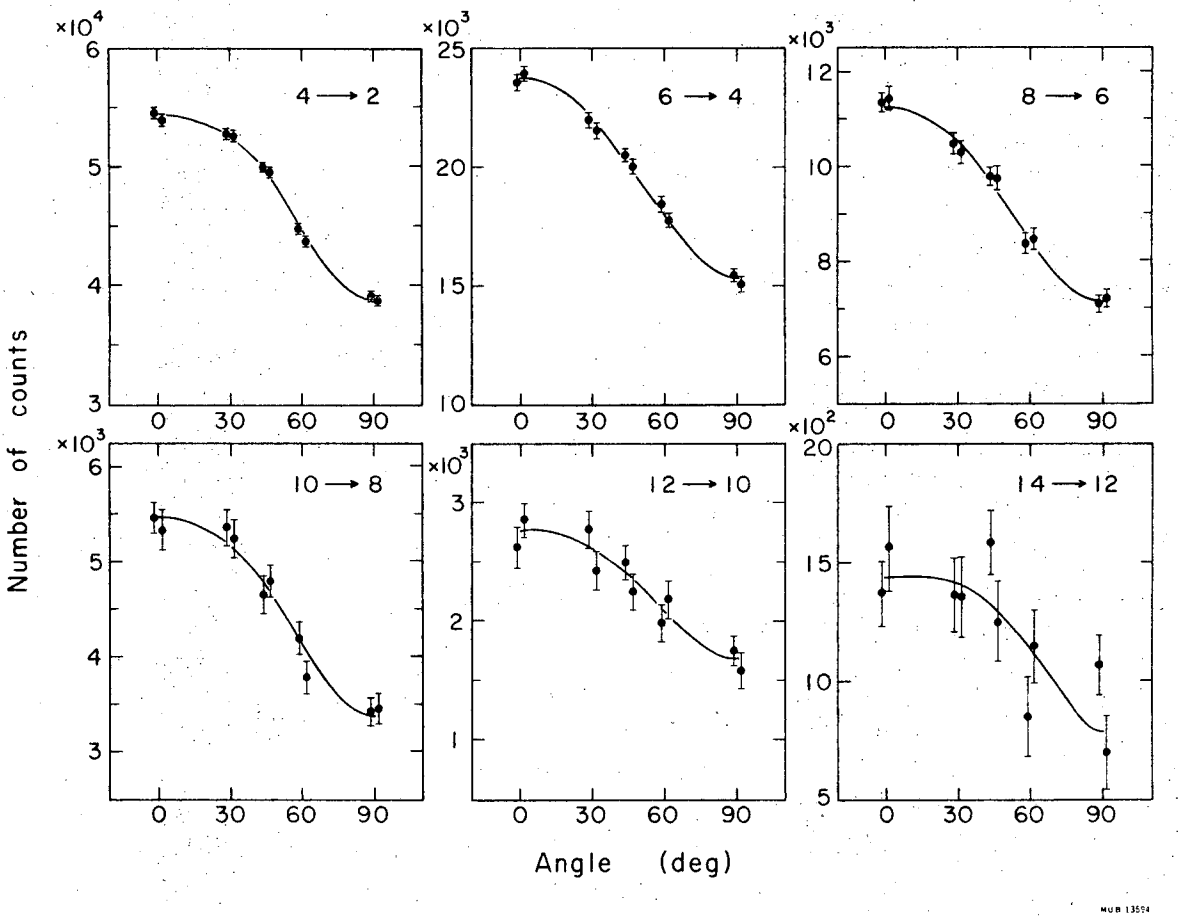
×10⁴
4 → 2
×10³
6 → 4
×10³
8 → 6
×10³
10 → 8
×10³
12 → 10
×10²
14 → 12
Number of counts
Angle (deg)
0
30
60
90
MUB 13594

Fig. 5

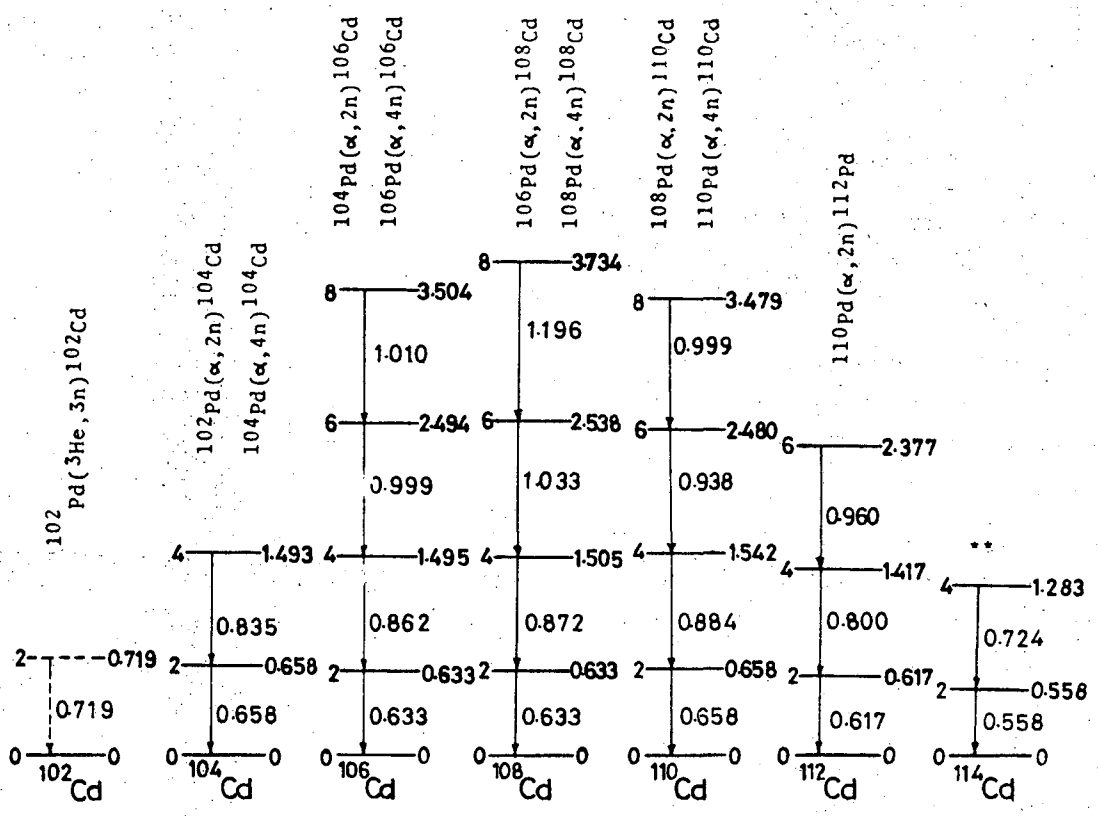

Fig.1

XBL697-3290

Fig. 6

^{124}Sn (^{40}A, 4n) $^{160}Er^*$ AT 150 MeV

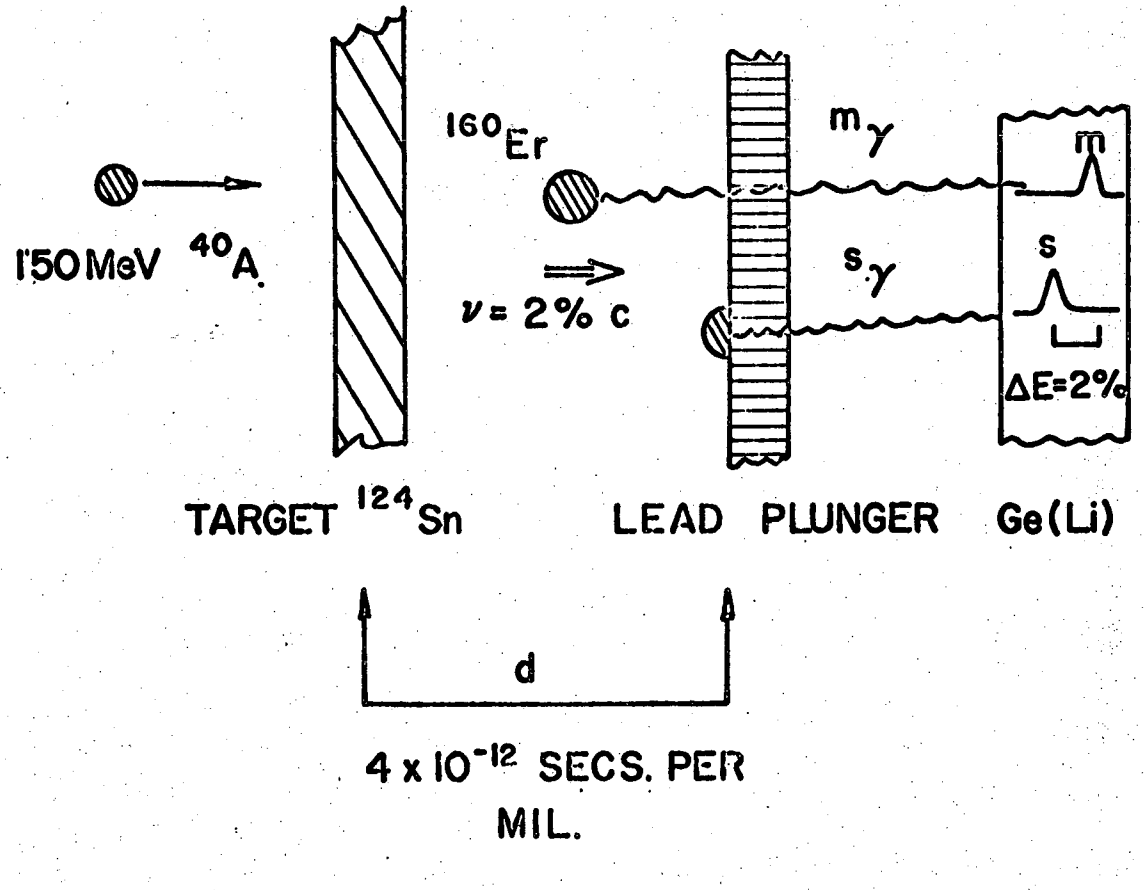

Fig. 7

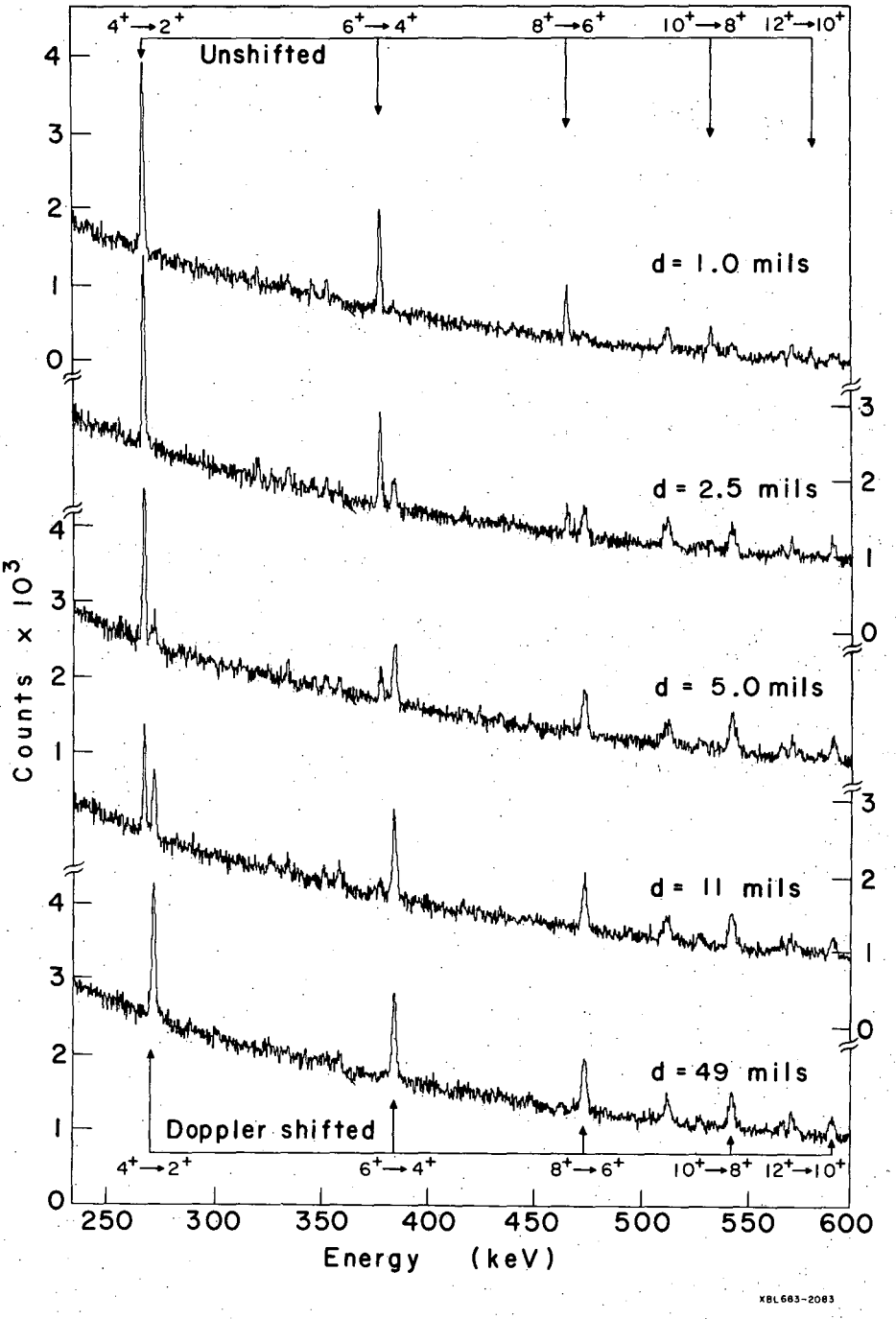
4+→2+
6+→4+
8+→6+
10+→8+
12+→10+
Unshifted
d = 1.0 mils
d = 2.5 mils
d = 5.0 mils
d = 11 mils
d = 49 mils
Doppler shifted
Counts x 10^3
Energy (keV)
250
300
350
400
450
500
550
600
XBL663-2083

Fig. 8

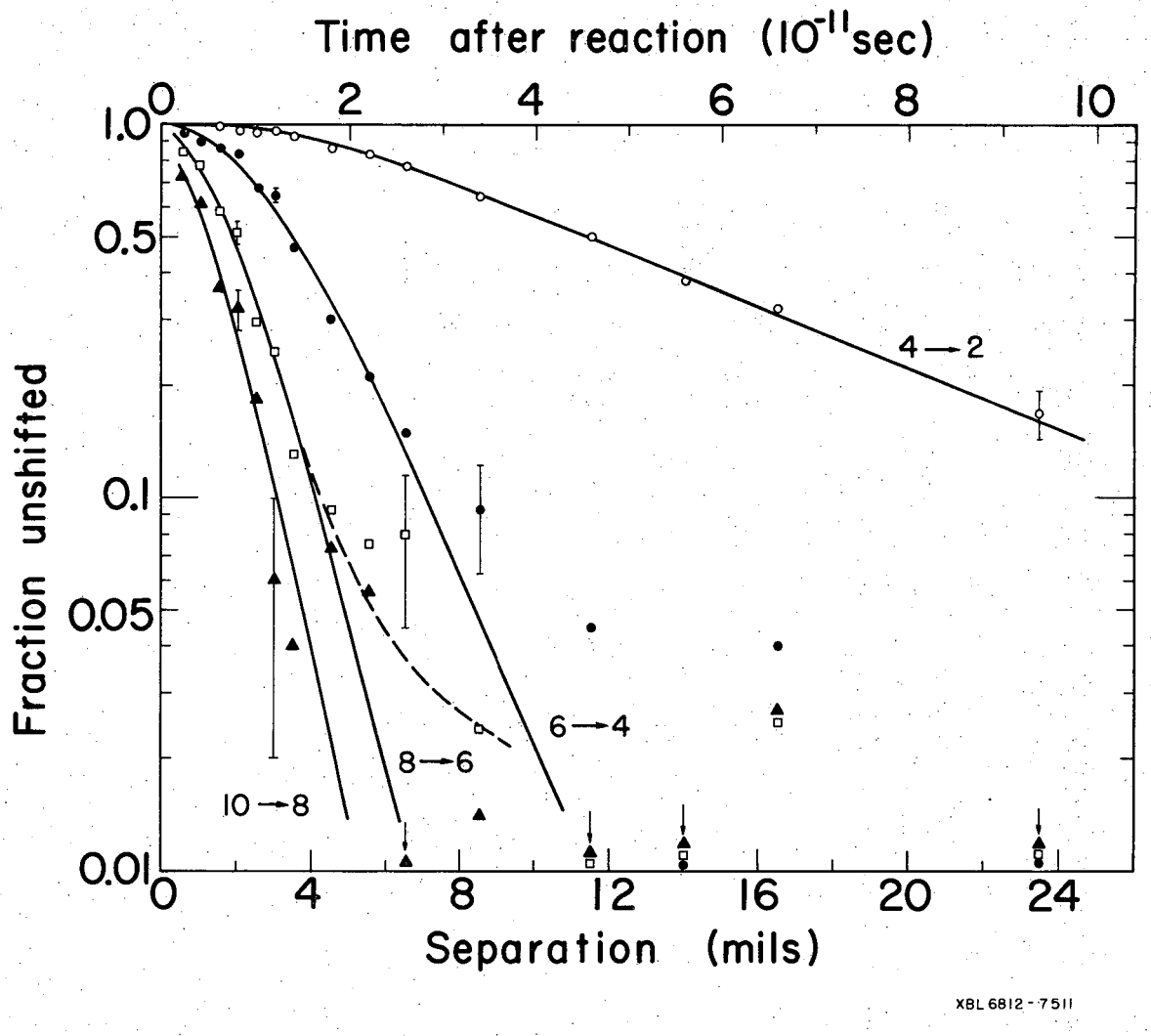
Time after reaction (10^{-11}sec)
0
2
4
6
8
10
1.0
0.5
0.1
0.05
0.01
Fraction unshifted
4→2
6→4
8→6
10→8
0
4
8
12
16
20
24
Separation (mils)
XBL6812-7511

Fig. 9

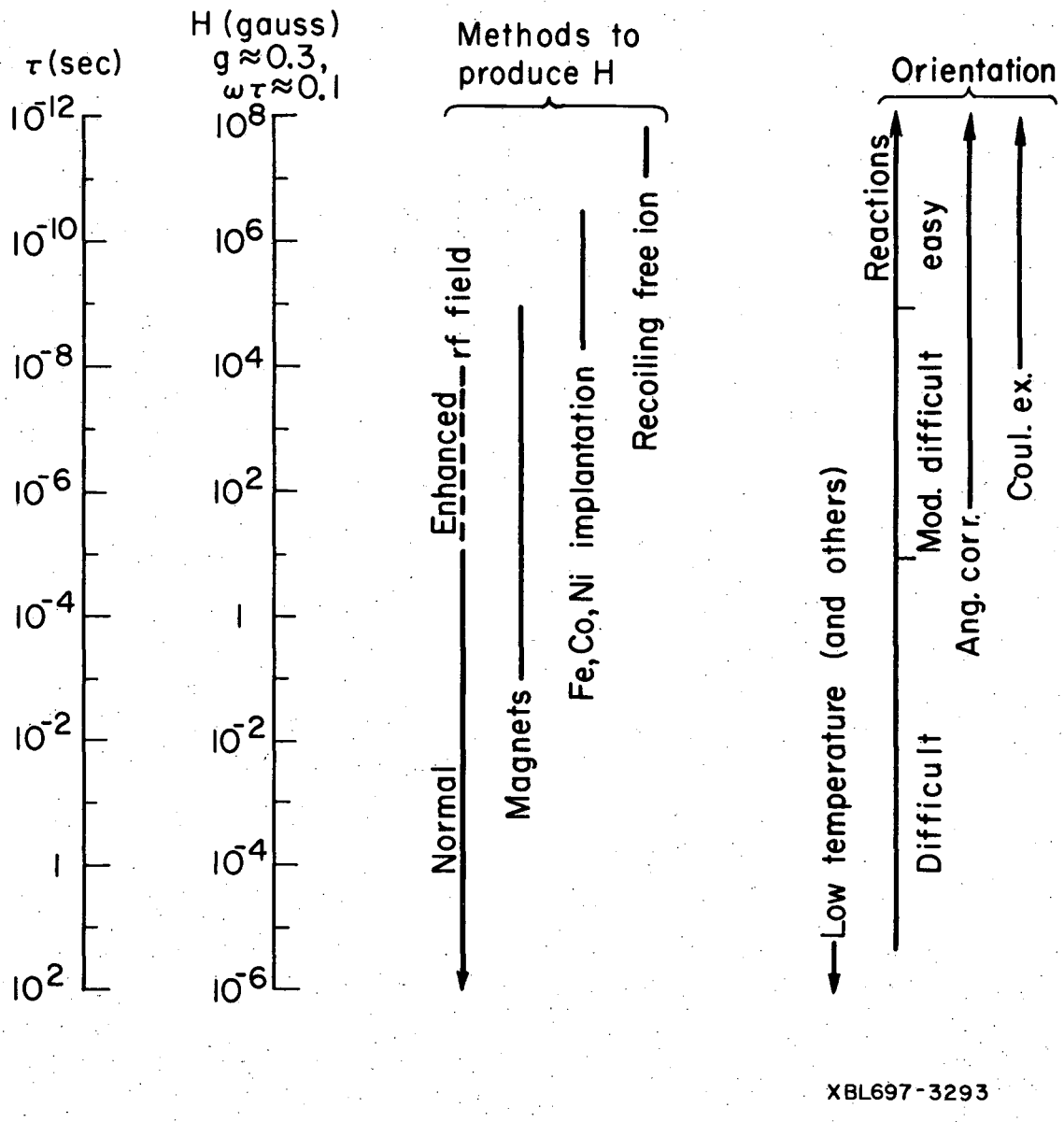
τ (sec)
H (gauss)
g ≈ 0.3,
ωτ ≈ 0.1
10^12
10^10
10^8
10^6
10^4
10^2
10^-2
10^-4
10^-6
Methods to produce H
Enhanced rf field
Normal
Magnets
Fe, Co, Ni implantation
Recoiling free ion
Orientation
Reactions
easy
Mod. difficult
Ang. corr.
Coul. ex.
Difficult
Low temperature (and others)
XBL697-3293

Fig. 10

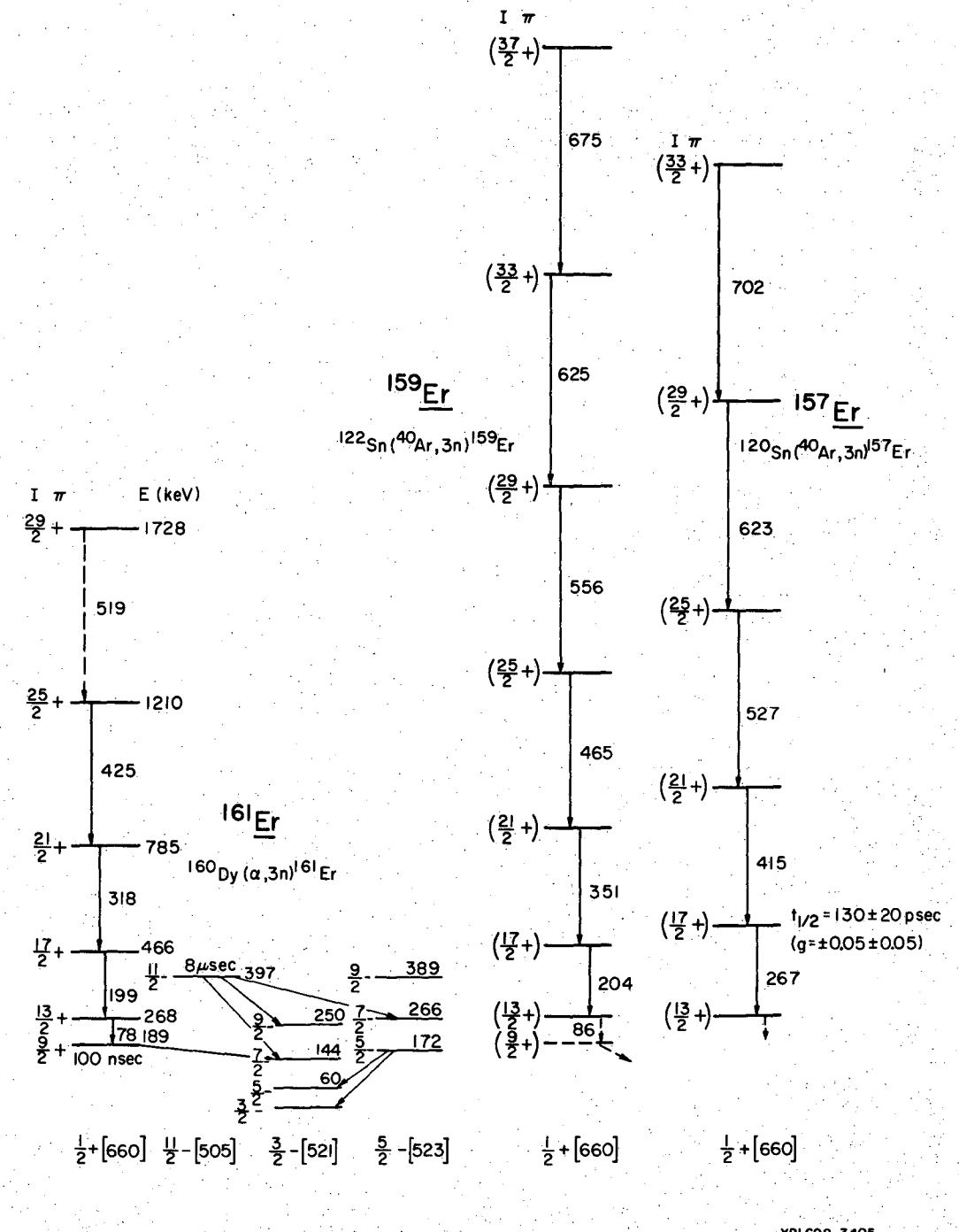
I π
(37/2+)
675
(33/2+)
625
(29/2+)
556
(25/2+)
465
(21/2+)
351
(17/2+)
204
(13/2+)
86
(9/2+)
159Er
122Sn(40Ar,3n)159Er
I π
(33/2+)
702
(29/2+)
157Er
120Sn(40Ar,3n)157Er
623
(25/2+)
527
(21/2+)
415
(17/2+)
t1/2 = 130 ± 20 psec
(g = ±0.05 ± 0.05)
267
(13/2+)
I π
E (keV)
29/2+ 1728
519
25/2+ 1210
425
161Er
160Dy (α,3n)161Er
21/2+ 785
318
17/2+ 466
199
13/2+ 268
78 189
9/2+ 100 nsec
11/2- 8μsec 397
9/2- 389
9/2 250
7/2- 266
7/2 144
5/2- 172
5/2 60
3/2
1/2+[660] 11/2-[505] 3/2-[521] 5/2-[523]
1/2+[660]
1/2+[660]
XBL698-3405

Fig. 11

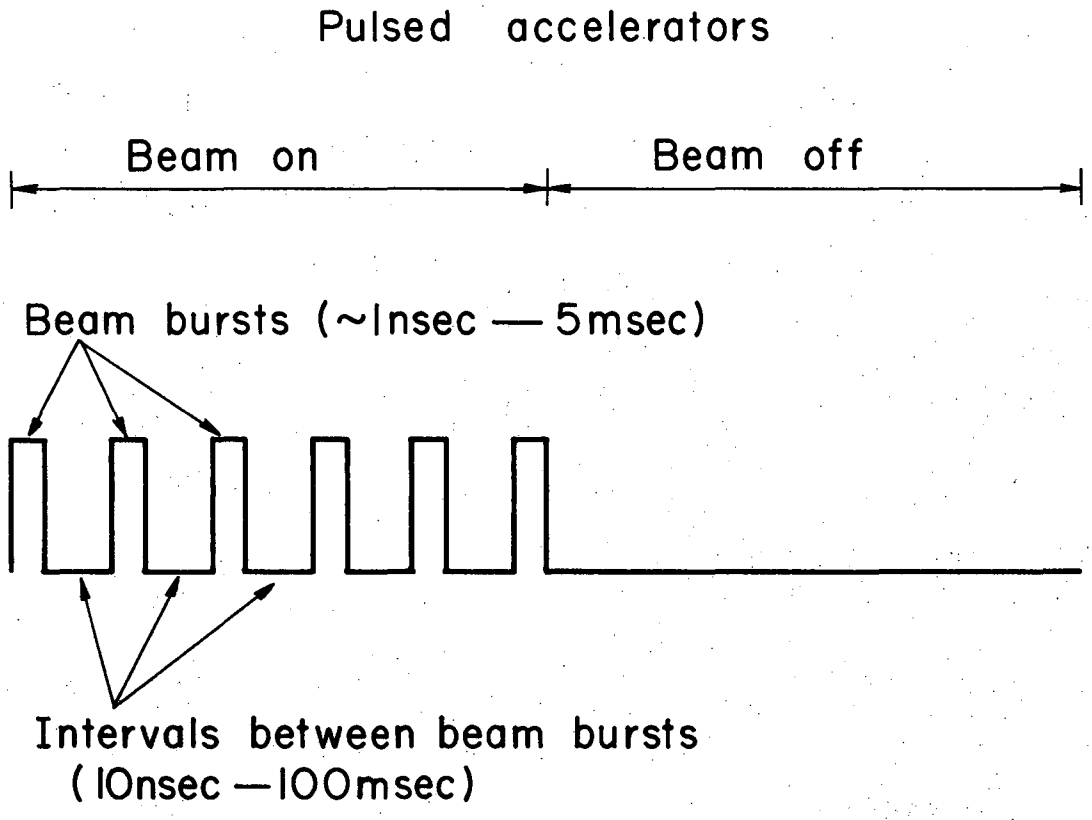

XBL698-3404

Fig. 12

TECHNICAL INFORMATION DIVISION
LAWRENCE RADIATION LABORATORY
UNIVERSITY OF CALIFORNIA
BERKELEY, CALIFORNIA 94720